Applied Catalysis A, General 598 (2020) 117550

Contents lists available at ScienceDirect

Applied Catalysis A, General

journal homepage: www.elsevier.com/locate/apcata

Rational design of bifunctional catalyst from KF and ZnO combination on alumina for cyclic urea synthesis from CO_2 and diamine

Nagendra Kulal[a,b], Crowny John[c], Ganapati V. Shanbhag[a,*]

[a] Materials Science and Catalysis Division, Poornaprajna Institute of Scientific Research (PPISR), Bidalur Post, Devanahalli, Bengaluru, 562 164, Karnataka, India
[b] Graduate Studies, Manipal Academy of Higher Education (MAHE), Manipal, 576104, Karnataka, India
[c] Chemistry Department, Christ University, Bengaluru, 560029, Karnataka, India

ARTICLE INFO

Keywords:
CO_2
Ethylenediamine
2-Imidazolidinone
Cyclic urea
Bifunctional catalyst

ABSTRACT

This study is mainly focused on the design of stable, active and selective catalyst for direct synthesis of 2-imidazolidinone (cyclic urea) from ethylenediamine and CO_2. Based on the rationale for the catalyst properties needed for this reaction, KF, ZnO and Al_2O_3 combination was selected to design the catalyst. ZnO/KF/Al_2O_3 catalyst was prepared by stepwise wet-impregnation followed by the removal of physisorbed KF from the surface. High product yield could be achieved by tuning acid-base sites by varying the composition and calcination temperature. The catalysts were characterized by various techniques like XRD, N_2-sorption, NH_3-TPD, CO_2-TPD, TEM, XPS and FT-IR measurements. It is shown that acidic and basic properties of the solvent can influence the activity and product selectivity for this reaction. Under optimized condition; 180 °C, 10 bar and 10 wt.% catalyst in batch mode, 96.3 % conversion and 89.6 % selectivity towards the 2-imidazolidinone were achieved.

1. Introduction

Carbon dioxide (CO_2) plays a vital role in increasing global warming ever since the industrial revolution had occurred. The burning of fossil fuels and coal paved the way for the increase of this greenhouse gas. This issue of global warming has been taken up seriously by scientists and they also warned the nations which release high content of carbon dioxide into the atmosphere. Since this has become a very important issue internationally, scientists are keen to reduce this greenhouse gas from the atmosphere. Carbon dioxide is non-toxic and abundantly available gas, can be utilized to produce several products like cyclic carbonates, carbamates, urethanes, substituted ureas, organic carbonates, methanol, and hydrocarbons. One such transformation is cycloaddition of CO_2 with a diamine to make cyclic urea. 2-imidazolidinone, a product of CO_2 and ethylenediamine (EDA) shows promising industrial applications such as an additive in plastics, intermediate in the synthesis of pharmaceuticals, agricultural chemicals [1]. This chemical is used in the manufacture of polymers and it is a finishing agent for textiles and leather. It is also used to formulate lacquers, plasticizers and adhesives and insecticides. As a formaldehyde remover, it can remove residual formaldehyde in fabrics treated by epoxy resin, 2D-resin painting, urea-formaldehyde resin, melamine formaldehyde resin, etc [2].

Conventionally, reactions of diamines with several kinds of reagents used as carbonyl sources such as phosgene, urea, organic carbonates [3,4], carbonyl selenide [5], carbonyldiimidazole [6], dithiocarbonate [7]. From the toxic point of these reagents, the reaction of a diamine with CO_2 provides a direct eco-friendly route for the synthesis of cyclic urea. Homogeneous catalysts for this reaction such as Ph_3SbO/P_4S_{10} [8] and $TBA_2[WO_4]$ [9] were reported as efficient catalysts but they possess several limitations including catalyst separation, recyclability and high cost of catalyst production. Arai [10] and Zhao [11] reported non-catalytic routes for direct synthesis of cyclic urea from CO_2 and diamine. However, these reactions were carried out under harsh conditions such as high temperature (≥200 °C), and pressure (≥6.0 MPa). There are very few reports on heterogeneous catalysts for this reaction in the previous literature. Among them, polyethylene-glycol-supported potassium hydroxide(KOH/PEG1000) [12] have been reported to be efficient catalysts for direct synthesis of cyclic urea from diamine and CO_2. This catalyst showed a low yield of cyclic urea (≤82 %), at a pressure of 80 bar CO_2 and 150 °C. CeO_2 [13] synthesized by biopolymer template method gave low yield for cyclic urea (≤ 37 %) at 7 bar CO_2 pressure and 160 °C. Among heterogeneous catalysts, Tomishige and co-workers reported pure commercial CeO_2 as the most efficient catalyst among different metal oxides such as ZnO, CaO, La_2O_3, TiO_2, MgO, ZrO_2, Pr_6O_{11} and Al_2O_3 [1]. Although CeO_2 catalyst shows promising catalytic activity for CO_2 and amine reaction and moreover, CeO_2 is an expensive chemical [14–20]. Based on this literature,

* Corresponding author.
E-mail address: shanbhag@poornaprajna.org (G.V. Shanbhag).

https://doi.org/10.1016/j.apcata.2020.117550
Received 22 October 2019; Received in revised form 27 March 2020; Accepted 1 April 2020
Available online 16 April 2020
0926-860X/ © 2020 Elsevier B.V. All rights reserved.

motivated to design a catalyst for the synthesis of 2-imidazolidinone from EDA and CO_2. Among the oxides tested, ZnO was reported to give 40 % conversion and 63 % selectivity and happened to be the second in the order of activity. This prompted us to check ZnO as an active ingredient in the catalyst system and further improve its activity by suitable modification. It is well known that CO_2 is activated by basic sites, whereas amines are activated by acidic sites. At the same time, stronger acidity may lead to deactivation of the catalyst by formation of polymeric products which also decreases selectivity for cyclic urea. By considering these aspects, the combination of ZnO and basic KF/Al_2O_3 was conceptualized for designing a catalyst for this reaction. There is only one report found in the literature on a catalyst KF/Zn(Al)O which was prepared by loading KF on calcined Zn-Al hydrotalcite and used as catalyst for transesterification of vegetable oil [21]. This material is different from $ZnO/KF/Al_2O_3$ taken in this study in terms of method of preparation, optimization of catalyst recipe as well as the reaction studied for this catalyst. Hence, there is a lot of scope to investigate $ZnO/KF/Al_2O_3$ as a material as such to investigate its physico-chemical properties and catalytic activity as a bifunctional catalyst. In the present study, the activity of ZnO was enhanced by supporting on KF/Al_2O_3 by wet impregnation method. KF/Al_2O_3 is a well-known solid base catalyst which has been applied as a catalyst for many organic reactions [22–24]. The loading of KF on Al_2O_3 creates new basic sites by the formation of potassium hydroxide and potassium hexafluoroaluminate (K_3AlF_6) and F^- species during preparation [22,25]. ZnO loading on KF/Al_2O_3 catalyst further creates the bifunctional property of acidity and basicity on its surface. It is shown in this study that the nature and number of active sites can be tuned by varying both ZnO and KF loading on γ-Al_2O_3 as well as calcination temperature for the synthesis of 2-imidazolidinone from EDA and CO_2. The catalyst has been characterized using various techniques including XRD, ICP-OES, BET, TPD, TEM, XPS and FT-IR. The reaction parameters have been optimized and solvent study has been conducted to achieve better yields for 2-imidazolidinone.

2. Experimental

2.1. Materials

Zinc nitrate hexahydrate, methanol and cerium (IV) oxide were purchased by Merck India Ltd. Potassium fluoride and EDA were procured from Loba Chemie Pvt. Ltd. Plural SB (pseudoboehmite) was procured from Sasol Germany GmbH.

2.2. Catalyst preparation

Pseudoboehmite was calcined at 550 °C for 4 h to get γ-Al_2O_3. Different weight percentages of ZnO and KF were loaded on γ-Al_2O_3 by wet impregnation method. In a typical procedure, 100 mL of an aqueous solution containing the required amount of KF was mixed with 20 g of γ-Al_2O_3 under constant rotation of 150 RPM in a rotary evaporator at 60 °C for 4 h and followed by evaporation of water. Then the sample was dried in an oven at 150 °C for 6 h and calcined at 550 °C for 4 h. After calcination, the catalyst was placed in 70 mL distilled water, stirred well and filtered to remove any physisorbed KF present on the catalyst, and dried at 200 °C. In a second step, a known amount of ZnO (from zinc nitrate precursor) was loaded on KF/Al_2O_3 by wet impregnation similar to the above procedure. Different amounts of ZnO and KF on Al_2O_3 catalysts are designated as (X)/ZnO/(Y) KF/Al_2O_3, where X and Y are mmol/g loading of ZnO and KF respectively (from measured values of Zn and K by ICP-OES).

2.3. Catalyst characterization

Powder X-ray diffraction (XRD) experiments were conducted over the 2θ range of 10–80° with steps of 0.02 and an interval of 0.5 s on X-ray diffractometer (Bruker D2 phaser) with Cu Kα radiation source and high-resolution Lynxeye detector. N_2 sorption experiments were performed at liquid nitrogen temperature 77 K after degassing the samples at 200 °C for 4 h under 10^{-2}kPa using Belsorb Mini (II) instrument (BEL Japan). The surface area, pore size, pore volume and N_2 adsorption-desorption isotherms of the catalyst were determined in this study. Temperature programmed desorption (TPD) studies were conducted on a Belcat-II (BEL Japan) instrument using NH_3 and CO_2 as probe molecules for acidity and basicity respectively. In a typical procedure, 0.1 g of sample was pretreated at 550 °C under He for 1 h in a quartz U- tube. The temperature was then decreased to 50 °C and 10 % NH_3 (CO_2) in He as adsorption gas was passed through the sample for 30 min with a flow rate of 30 mL/min. The physisorbed NH_3 (or CO_2) gas was then removed by purging with He gas for 15 min. TPD test was carried out by heating sample up to 600 °C at a rate of 10 °C/min under constant flow of He (30 mL/min) using TCD detector. The elemental composition of the catalysts was measured by ICP-OES (Perkin Elmer). Transmission electron microscopy (TEM) and high-resolution transmission electron microscopy (HRTEM) techniques were used to determine the morphology of the catalysts using JEM-2100 (JEOL) instrument at an accelerating voltage of 200 kV. X-ray photoelectron spectroscopy (XPS) analysis was performed on Kratos Axis Ultra DLD using Al Kα radiation dual anode source (Energy, hυ = 1486.6 eV). The carbon (C 1s) peak (284.8 eV) was used as the reference to calibrate the binding energy of all XPS peaks. Fourier transform infrared (FT-IR) spectra were recorded using the Bruker Alpha T in the 400 – 4000 cm^{-1} range by using KBr pellets. Elemental analysis for Zn and K was conducted for leaching study from Perkin Elmer AAnalyst 200 atomic absorption spectrometer (AAS) using zinc nitrate and potassium nitrate standard solutions as references respectively.

2.4. Catalytic activity studies

The carbonylation reaction of EDA with CO_2 to make 2-imidazolidinone was performed in a mechanically stirred 100 mL high-pressure stainless steel reactor (Amar Equipments Pvt. Ltd., India). In a typical procedure, reactant EDA was taken in a methanol solvent in the reactor and the catalyst was added to it. The reactor was then tightened and pressurized with CO_2 from the cylinder connected to the gas inlet valve of the reactor. The reactor was equipped with pressure gauge, furnace and thermocouple to monitor the reaction temperature at a given time. The reaction mixture was stirred during the reaction with a speed of 700 rpm. After completion of the reaction, the stirring and heating were stopped and the reactor was immersed in an ice bath to condense the vapors completely. The excess CO_2 gas was vented out (after the gas analysis) and the liquid product was centrifuged to separate the catalyst from the rest. The liquid sample thus obtained was analyzed by an Agilent 7890B GC with HP-5 column and FID detector. The gas sample was obtained from the outlet of the reactor and analyzed by Thermo Scientific Trace GC-700 equipped with a packed column (Porapak Q) and TCD detector.

$$X_{EDA}(\%) = \frac{X_{EDA(i)} - X_{EDA(f)}}{X_{EDA(i)}} \times 100$$

$$Y_{2-imidazolidone}(\%) = \frac{X_{2-imidazolidone}}{X_{EDA(i)}} \times 100$$

Where X_{EDA} and $Y_{2-imidazolidone}$ are EDA conversion and 2-imidazolidinone yield respectively. $X_{EDA(i)}$ and $X_{EDA(f)}$ correspond to initial and final molar concentrations of EDA respectively. $X_{2-imidazolidone}$ is the molar concentration of 2-imidazolidinone formed in the reaction.

In order to understand if any active species of the catalyst were leached into the reaction mixture, a leaching test was performed for the synthesis of 2-imidazolidinone from EDA and CO_2. The reaction was stopped after 1 h and the reaction mixture was cooled down and depressurized by releasing the gases slowly. The catalyst was separated

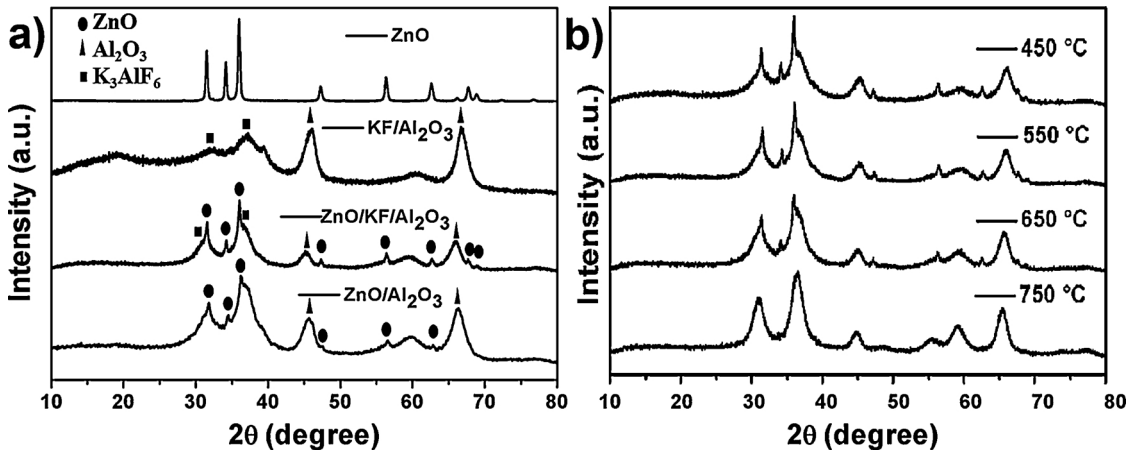

Fig. 1. XRD patterns of a) ZnO (550 °C), KF/Al_2O_3 (550 °C), $ZnO/KF/Al_2O_3$ (550 °C) and ZnO/Al_2O_3 (550 °C); b) $ZnO/KF/Al_2O_3$ calcined at different temperatures.

from the reaction mixture by centrifugation and the reaction was continued with the supernatant using fresh CO_2 in the high pressure reactor.

Recyclability studies were also carried out at 160 °C, 10 bar pressure for 4 h. After the first run, the catalyst was filtered out from the reaction mixture and washed thoroughly with solvent acetone. The catalyst was then dried at 120 °C overnight and finally calcined at 550 °C for 4 h. This procedure was applied to all the successive runs confirm the regeneration of the catalyst before each cycle.

3. Results and discussion

3.1. Characterization

3.1.1. X-ray powder diffraction patterns

XRD patterns of ZnO and KF loaded on γ-Al_2O_3 (2.40ZnO /0.49 K F/ Al_2O_3) was compared with its precursors with same loading, ZnO, KF/ Al_2O_3 and ZnO/Al_2O_3 as shown in Fig. 1. Pure ZnO calcined at 550 °C showed sharp crystalline peaks corresponding to its different phases. KF/Al_2O_3 (550 °C) was relatively less crystalline and contained peaks corresponding to Al_2O_3 phase and a new phase corresponding to K_3AlF_6 was formed by the interaction of KF with support γ-alumina [21]. The excess of KF on the support was removed by treating calcined catalyst with water. The XRD diffractions characteristic of KF was not found in the XRD pattern of KF/Al_2O_3 catalyst.

$$12\,KF + Al_2O_3 + 3H_2O \rightarrow 2K_3AlF_6 + 6K^+ + 6OH^- \quad (1)$$

OH^- was produced during the reaction when KF loaded on γ- Al_2O_3 support as shown in Eqn. 1. The XRD pattern of ZnO loaded on KF/ Al_2O_3 exhibited ZnO phase along with K_3AlF_6 phase. Also, all the phases of $ZnO/KF/Al_2O_3$ corresponding to ZnO and Al_2O_3 were present in ZnO/Al_2O_3 accept two minor peaks at 67.7° and 68.8°. The lower intensity of the Al_2O_3 peaks in $ZnO/KF/Al_2O_3$ compared with ZnO/ Al_2O_3 is because of the formation of additional K_3AlF_6 phase in the former which decreased the concentration of alumina in the catalyst. Fig. 1b shows XRD patterns of $ZnO/KF/Al_2O_3$ calcined at different temperatures from 450 to 750 °C. The crystallinity of the material increased with an increase in calcination temperature from 450 to 750 °C.

3.1.2. N_2 sorption studies

Effect of surface area and pore volume of $ZnO/KF/Al_2O_3$ catalysts were analyzed by nitrogen adsorption-desorption (Fig. 2). N_2 sorption of γ-Al_2O_3, and KF/Al_2O_3 and $ZnO/KF/Al_2O_3$ catalysts showed type IV isotherm with H2 type hysteresis loop, which indicated that these samples possessed mesoporous structure (Fig. 2a). The relative pressure increased > 0.65 sharply due to capillary condensation of nitrogen within uniform pores. BJH plots confirmed the presence of mesoporosity with an average mesopore size of 22 nm. The plots show that the modification of γ-Al_2O_3 with KF and ZnO did not affect its mesoporous structure but surface area decreased (Fig. 2b). After loading of ZnO on the KF/Al_2O_3, the BJH plot showed split into two but it doesn't affect the mesoporous structure of support (γ-Al_2O_3) and surface area was decreased. N_2 sorption isotherm conforms the mesoporosity in $ZnO/KF/Al_2O_3$ which was retained after modification of mesoporous Al_2O_3. The surface area of γ-Al_2O_3, KF/Al_2O_3 and ZnO/KF/ Al_2O_3 are 198.16, 175.73 and 110.80 m^2/g respectively.

3.1.3. Transmission electron microscopy

The morphology of $ZnO/KF/Al_2O_3$ catalyst was revealed by TEM analysis (Fig. 3). The KF/Al_2O_3 shows (Fig. 3a) interconnected rod-like particles with length in the range of 10–35 nm, which is very similar to γ- Al_2O_3 [26]. Along with rod-like particles, thin flake shaped particles stacked in a disordered manner were also observed. These flakes are randomly oriented with respect to the electron beam direction. It is also apparent from the high resolution images that the shape of flakes are formed by the aggregation of particles and there is no structure within the flakes. ZnO loaded on the KF/Al_2O_3 showed spherical particles of ZnO along with nanorods of KF/Al_2O_3 (Fig. 3b). The HRTEM of the $ZnO/KF/Al_2O_3$ also shows the existence of the spherical ZnO and rod-like KF/Al_2O_3 particles (Fig. 3c). The SAED patterns of KF/Al_2O_3 and $ZnO/KF/Al_2O_3$ samples were indexed to the corresponding planes and well-matched with the XRD pattern. It can be noted that the SAED pattern ring distance 7.10/nm corresponds to (440) plane of γ-Al_3O_3 phase (Fig. 3d). The SAED pattern distance of 3.43/nm and 5.91/nm correspond to (100) and (110) planes of ZnO respectively (Fig. 3e).

3.1.4. Chemisorption measurements

Temperature programmed desorption (TPD) method is used mainly to quantify acidic, basic sites and their strength of the distribution. TPD temperature profiles suggested that ZnO and KF on Al_2O_3 with different loadings contained mainly weak and medium acid and basic sites with peak max. > 200 °C and 200 – 400 °C respectively (Figs. 4 and 5). Acidity and basicity of pure γ-Al_2O_3 without modification is 0.27 and 0.09 mmol/g respectively. Upon loading of 0.53 mmol/g of KF decreased acidity to 0.21 mmol/g, whereas basicity increased to 0.13 mmol/g (Table 1). This is because K_3AlF_6 crystal phase and OH^- ions were generated from the reaction between KF and γ-Al_2O_3 (Fig. 1). ZnO loading directly on Al_2O_3 resulted in 0.20 mmol/g of acidity and 0.11 mmol/g of basicity. The total acid and basic sites were found to be higher for $ZnO/KF/Al_2O_3$ compared to ZnO/Al_2O_3 with the same amount of ZnO loading. The comparison of TPD profiles shows that the combination of ZnO and KF on Al_2O_3 generates more weaker acidic and basic sites compared to independent loadings in ZnO/Al_2O_3 and KF/ Al_2O_3 catalysts [Fig. 6]. The molar concentration of KF was varied from

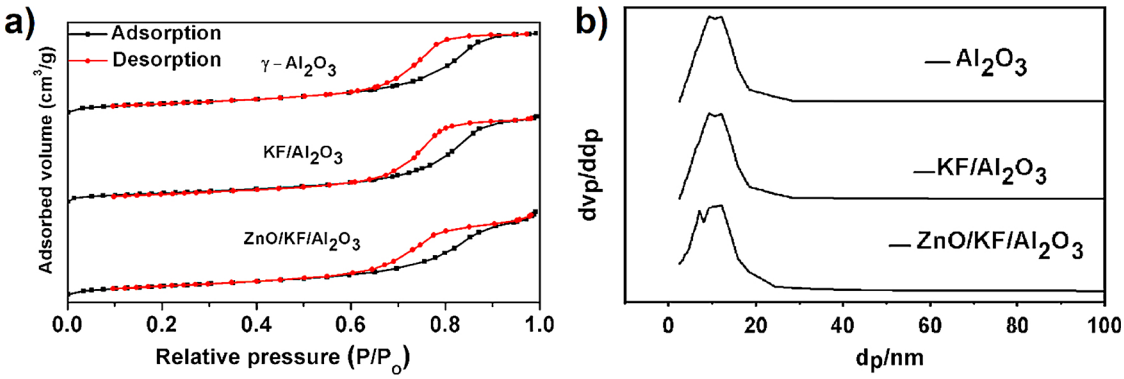

Fig. 2. a) Nitrogen physisorption isotherms and b) BJH pore size distribution for γ-Al_2O_3, KF/Al_2O_3 and ZnO/KF/Al_2O_3.

0.35 to 0.53 mmol/g keeping ZnO loading constant (2.4 mmol/g) in ZnO/KF/Al_2O_3. As the concentration of KF increased from 0.35 to 0.53 mmol/g, acidity decreased from 0.25 to 0.18 mmol/g, whereas basicity increased from 0.10 to 0.14 mmol/g. However, the strength of acidity and basicity remained almost the same as shown in corresponding TPD plots (Fig. 4). This clearly confirms the generation of basicity upon the interaction of KF and Al_2O_3 as mentioned earlier. Also, ZnO loading was varied from 1.15 to 3.34 mmol/g on 0.53 K F/Al_2O_3 which resulted in a change in the acid-base property of the catalyst (Table 1) (Fig. 5). Interestingly, both acidity and basicity increased with increase in ZnO loading on KF/Al_2O_3 (from 0.11 to 0.21 mmol/g and 0.10 to 0.16 mmol/g respectively) which could be due to the generation of new acid and basic sites upon the interaction of ZnO with Al_2O_3 support [27]. The ZnO/KF/Al_2O_3 with optimized composition was calcined at different temperatures to tune the acid and base sites further. As the calcination temperature was increased from 450 to 750 °C, the acidity decreased but there was an increase in basicity. This could be due to an increase in the formation of K_3AlF_6 and OH^- phases upon an increase in calcination temperature (Table 2). The decrease in acidity can be attributed to a decrease in acidic alumina phases due to its interaction with KF. It can be seen in TPD plots (Fig. 7) that new high strength acidic and basic sites were formed at ≥ 650 °C calcination temperature which could be due to the generation of coordinatively unsaturated species on the catalyst surface.

3.1.5. X-ray photoelectron spectroscopy (XPS)

XPS analyses of 2.03ZnO/Al_2O_3, 0.53 K F/Al_2O_3 and 2.40ZnO/0.49 K F/Al_2O_3 catalysts were performed to understand the actives sites present in the catalyst. Fig. 8 shows the XPS spectra of Zn 2p core level of 2.03ZnO/Al_2O_3 and 2.40ZnO/0.49 K F/Al_2O_3 catalysts. The binding

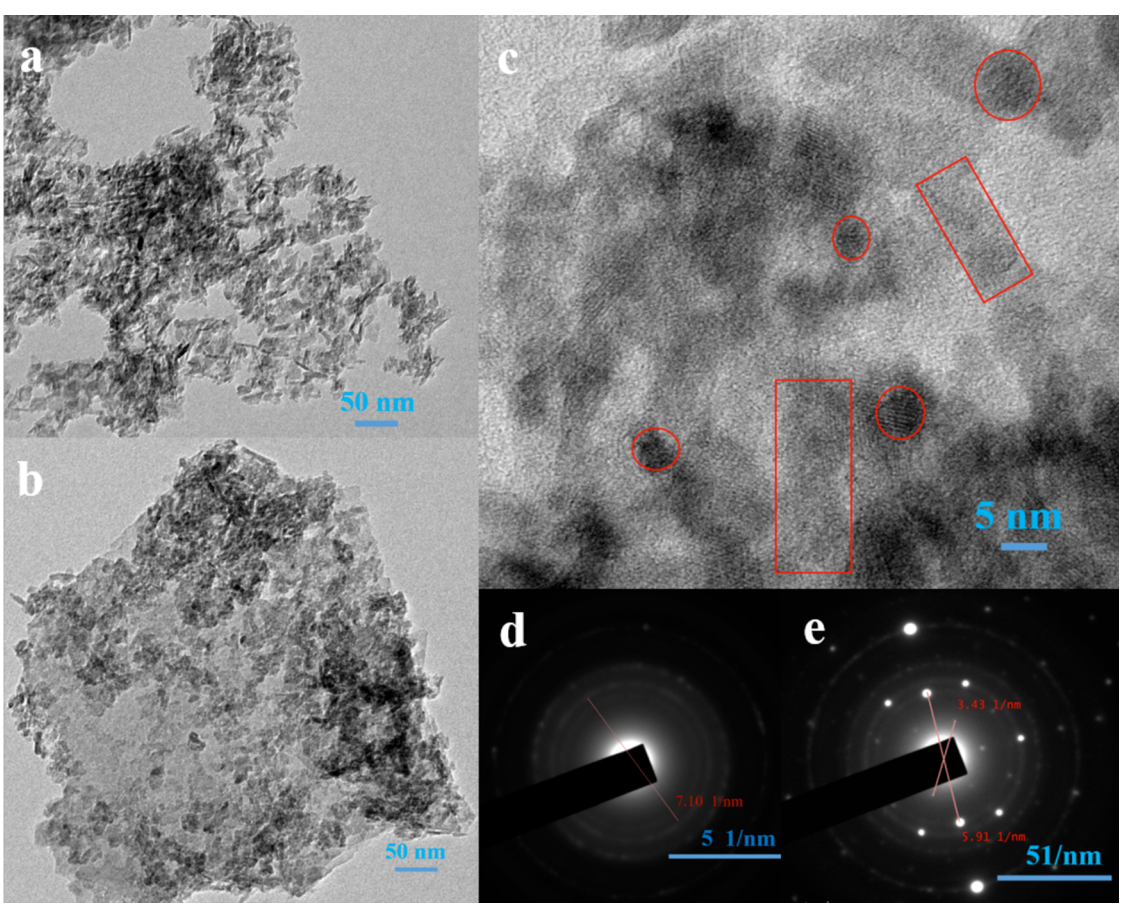

Fig. 3. TEM images of (a) KF/Al_2O_3 and (b) ZnO/KF/Al_2O_3, (c) HRTEM image of ZnO/KF/Al_2O_3, SAED patterns of (d) KF/Al_2O_3 and (e) ZnO/KF/Al_2O_3.

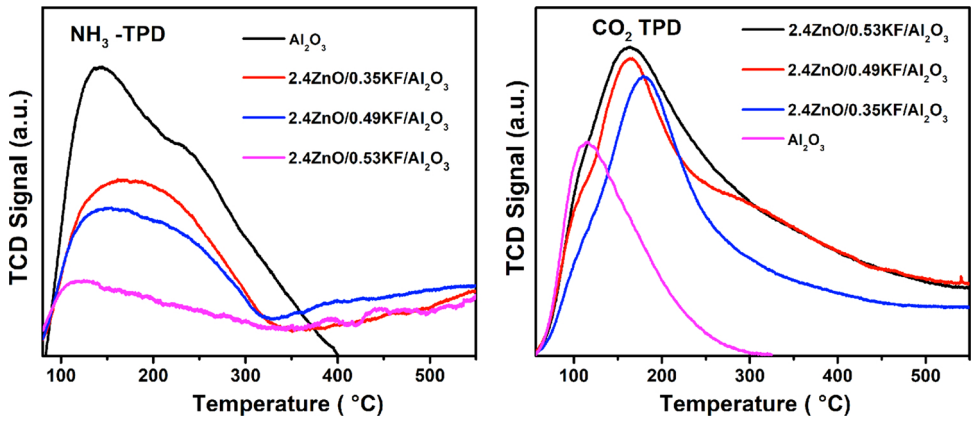

Fig. 4. NH_3–CO_2 TPD profiles of different concentrations of KF in ZnO/KF/Al_2O_3 catalyst calcined at 550 °C.

energies from 1020 to 1027 eV and 1043–1050 eV are assigned to Zn $2p_{3/2}$ and Zn $2p_{1/2}$ spin orbitals respectively. Interestingly, the spectra showed a major difference in the number of components corresponding to Zn 2p spin orbitals. The fitted peaks centered at 1021.5 and 1044.6 eV are assigned to Zn^{2+} ion of tetrahedral structure [28]. The peaks at 1024.0 and 1047.6 eV observed only for 2.40ZnO/0.49 K F/Al_2O_3 catalyst are assigned to Zn^{2+} octahedral structure [29,30].

Fig. 9 depicts the Al 2p XPS core spectra of 2.03ZnO/Al_2O_3, 0.53 K F/Al_2O_3 and 2.40ZnO/0.49 K F/Al_2O catalysts. The Al 2p spectra of 2.03ZnO/Al_2O_3 contained 2 peaks at 73.6 and 74.2 eV which are assigned to Al^{3+} ions occupying the tetrahedral [AlO_4], and octahedral Al_2O_3 respectively [29,31]. Al 2p peaks in 0.53 K F/Al_2O_3 catalyst with binding energies of 73.6 and 75.6 eV are assigned to Al^{3+} ions occupying Al_2O_3 and K_3AlF_6 phases respectively [32]. The K_3AlF_6 phase was formed by the reaction of KF and Al_2O_3 which is also evident in XRD analysis (Fig. 1). ZnO loaded on KF/Al_2O_3 shows Al^{3+} located at 74.2 and 75.6 eV for tetrahedral [AlO_4] and K_3AlF_6 respectively [29,32]. Al_2O_3 phase is present in both ZnO/Al_2O_3 and KF/Al_2O_3 catalysts, but after the loading of ZnO on KF/Al_2O_3 catalyst, Al_2O_3 phase at 73.6 eV vanished and new tetrahedral [AlO_4] phase at 74.2 eV is formed.

Fig. 10 shows the O 1s spectra of a) 0.53KF/Al_2O_3 b) 2.03ZnO/Al_2O_3 and 3) 2.40ZnO/0.49 K F/Al_2O_3 catalysts containing two kinds of oxygen contributions at binding energies of 530.0 and 531.4 eV. The peak at 530.0 eV is associated to the lattice oxygen of metal [33], whereas 531.4 eV peak is attributed to the coordinatively unsaturated surface $O^{\delta-}$ [31,34]. The Oδ- on the surface activates the reactant molecules which improves the catalytic performance. The ratio of the lattice oxygen to the surface Oδ- in these three catalysts indicates that the surface Oδ- species in ZnO/KF/Al_2O_3 is more than that of ZnO/Al_2O_3 and KF/Al_2O_3 catalysts. This clearly indicates the formation of more defect sites due to the interaction of ZnO and KF on Al_2O_3 support.

3.2. Catalytic activity studies

EDA reacts with CO_2 to readily produce dicarbamic acid without a catalyst at room temperature [1]. Dicarbamic acid is usually unstable at higher temperatures which either decompose or converts into a carbamate (the intermediate of the desired product). The catalyst with acid-base bifunctional property is suitable for this reaction as basic sites activate intermediate carbamic species by an abstraction of the proton, whereas acid sites activate the amine group (Scheme 1).

Initially, the reaction was carried out under conditions; 160 °C, 10 bar CO_2, 1.2 g of EDA and solvent methanol with catalyst precursors like Al_2O_3, KF/Al_2O_3 and ZnO/Al_2O_3 which gave 6.1, 13.7 and 24.7 % yield for 2-imidazolidinone respectively (Table 1). Higher selectivity of 98.0 % for KF/ Al_2O_3 shows that basicity in the catalyst enhances carbonylation reaction. Higher conversion of 26.8 % and good selectivity of 92.2 % for ZnO/ Al_2O_3 compared to pure γ-Al_2O_3 indicates the importance of ZnO role in carbonylation of diamine with CO_2. Thus both KF and ZnO independently enhanced the activity of Al_2O_3 in spite of the difference in nature of active sites generated due to them and which is also evident in XPS analysis and FT-IR adsorption study. This prompted us to work further on the combination of both KF and ZnO for their synergistic effect upon loading onto γ-Al_2O_3. To understand the effect of ZnO loading, different concentrations of ZnO from 1.15 to 3.34 mmol/g were loaded on 0.53 K F/Al_2O_3 and screened for carbonylation reaction under identical condition (Table 1). As the concentration of ZnO increased from 1.15 to 2.40 mmol/g, the yield increased substantially from 23.4–56.4% and then decreased to 45.8 %

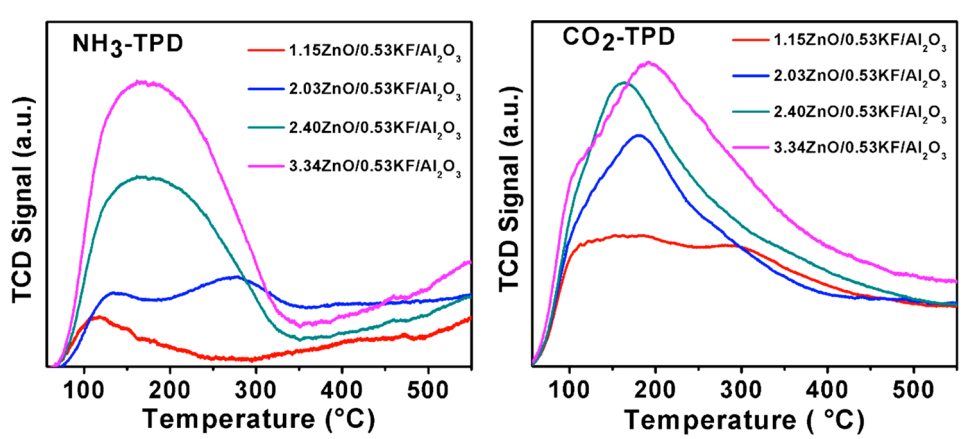

Fig. 5. NH_3 – CO_2 TPD profiles of different concentrations of ZnO in ZnO/KF/Al_2O_3 catalyst calcined at 550 °C.

Table 1
Physicochemical properties and catalyst testing of $ZnO/KF/Al_2O_3$.

Catalyst	KF loading (mmol/g)		ZnO loading (mmol/g)		Surface area (m^2/g)	Acidity (mmol/g)	Basicity (mmol/g)	Total acid-base sites (mmol/g)	Reaction result[b]			
	Initial	Final[a]	Initial	Final[a]					Conv. of EDA (%)	Sel. for cyclic urea (%)	Yield of cyclic urea (%)	[c]Yield of major side product
None	–	–	–	–	–	–	–	–	1.3	73.0	0.95	Trace
γ-Al_2O_3	–	–	–	–	198.2	0.31	0.09	0.40	6.7	91.1	6.1	0.4
0.53 K F/Al_2O_3	5.2	0.53	–	–	175.73	0.21	0.13	0.34	15.4	98.0	13.7	0.2
2.03ZnO/Al_2O_3	–	–	3.68	2.4	146.3	0.20	0.11	0.31	26.8	92.2	24.7	1.6
Changing the loading of KF in ZnO/KF/Al_2O_3												
2.40ZnO /0.35 K F/Al_2O_3	1.7	0.35	3.7	2.4	132.14	0.25	0.10	0.35	43.7	95.8	41.8	1.3
2.40ZnO /0.49 K F/Al_2O_3	3.4	0.49	3.7	2.4	133.42	0.23	0.13	0.36	72.9	98.0	71.4	1.2
2.40ZnO /0.53 K F/Al_2O_3	5.2	0.53	3.7	2.4	122.99	0.18	0.14	0.32	60.0	94.0	56.4	3.0
Changing the loading of ZnO in ZnO/KF/Al_2O_3												
1.15ZnO /0.53 K F/Al_2O_3	5.2	0.53	1.2	1.15	171.73	0.11	0.10	0.21	23.8	98.5	23.4	0.3
2.03ZnO /0.53 K F/Al_2O_3	5.2	0.53	2.4	2.03	139.66	0.15	0.12	0.27	38.5	98.0	37.7	0.6
2.40ZnO /0.53 K F/Al_2O_3	5.2	0.53	3.7	2.40	122.99	0.18	0.14	0.32	60.0	94.0	56.4	3.0
3.34ZnO /0.53 K F/Al_2O_3	5.2	0.53	4.9	3.34	110.84	0.21	0.16	0.37	51.3	89.4	45.8	4.6

[a] Measured value of K by ICP-OES after water treatment to remove physisorbed KF.
[b] Reaction condition: 1.2 g of EDA 10 wt. % of catalyst w.r.t EDA, 10 bar CO_2 pressure, 160 °C for 4 h, 3.2 g of methanol as solvent. [c]methylimidazolidin-2-one.

upon further increase in loading. Increase in the product yield can be attributed to the increase in total acid and base sites upon increase of ZnO loading in the catalyst (Fig. S1). As ZnO loading was increased beyond a certain concentration, it produced more polymeric side products which decreased both conversions (due to catalyst deactivation) and selectivity in this reaction.

As the concentration of KF increased from 0.35 to 0.49 mmol/g, the yield increased from 41.8–71.4%. Further increase in KF to 0.53 mmol/g, decreased the yield to 56.4 % which could be attributed to the lower amount of acid sites (Table 1, Fig. S1). It can be seen from TPD profile (Fig. 4) that there was a substantial decrease in acidity with increase in KF loading to 0.53 mmol/g. Among all the combinations of ZnO and KF on Al_2O_3, 2.4 mmol/g of ZnO and 0.49 mmol/g of KF loading on Al_2O_3 were found to be optimum for this reaction

2.40ZnO/0.49 K F/Al_2O_3 calcined from 450 to 750 °C were used as catalysts in carbonylation reaction to tune the acidic and basic sites to achieve high product yield. As the calcination temperature increases from 450 to 550 °C, the conversion of EDA increased from 68.6–72.9%. Further increase in the calcination temperature, decreased the EDA conversion to 63.3 %. As the calcination temperature increased the acidity decreased, whereas basicity increased (Table 2). This is because there was an increase in K_3AlF_6 crystal phase and OH– with an increase in calcination temperature from the reaction between KF and γ-Al_2O_3. At 550 °C calcination temperature, the right combination of acid and base sites could be responsible for highest yield for 2-imidazolidinone product.

3.2.1. Influence of reaction parameters

The catalyst loading into the reactor was the percentage of the catalyst with respect to the weight of the reactant (EDA) and the results are illustrated in Fig. 11. The synthesis of 2-imidazolidinone was studied with different amounts of 2.4ZnO/0.49 K F/Al_2O_3 catalyst at 160 °C, 10 bar CO_2 pressure (CO_2/EDA = 2) for 4 h. As the concentration of catalyst increased from 5 to 10 wt.%, EDA conversion increased from 42 to 72.4 %. Further, increase in catalyst weight from 10 to 20 wt.% resulted in only a marginal improvement in conversion. The selectivity for 2-imidazolidinone decreased marginally (by 4.1 %) as catalyst loading was increased from 5 to 20 wt. % due to the formation of side product, methylimidazolidin-2-one.

The synthesis of 2-imidazolidinone from EDA and CO_2 was investigated at different reaction temperatures to optimize the condition to achieve high product yield (Fig. 12). The EDA conversion was 34 % at 150 °C which increased substantially to 74 % with an increase by10 °C. Later, there was a slow increase in conversion with an increase in temperature and it reached 98 % at 190 °C. At 180 °C, conversion of EDA and selectivity for 2-imidazolidinone were 96.3 and 96.1 % respectively. Further, an increase in temperature to 190 °C, the conversion of EDA increased marginally, whereas selectivity for 2-imidazolidinone decreased with increase in side product formation. Hence, 180 °C was taken as an optimum reaction temperature for further study.

The reaction was carried out at different pressures to study its effect on the conversion and selectivity for 2-imidazolidinone (Fig. 13). As CO_2 is a reactant, varying the pressure also alters CO_2: EDA mole ratio. For this study, all the experiments were carried out respect wt.% of catalyst loading, 180 °C and 4 h. It can be observed from Fig. 13. That an increase in CO_2 pressure from 5 bar to 10 bar (or CO_2/EDA = 1–2), increased the EDA conversion. At 10 bar pressure, the conversion of EDA and selectivity for 2-imidazolidinone was 96.3 and 96.1 % respectively. The increase in the CO_2 concentration increases the availability of CO_2 for the reaction and increase in pressure brings the molecules closer to facilitate the reaction. However, further, increase in the CO_2 pressure to 15 bar resulted in lower EDA conversion probably due to the blockage of basic sites of the catalyst by adsorption of acidic CO_2 at higher pressures.

The carbonylation reaction was studied with respect to time from 2 to 8 h at a reaction temperature of 180 °C and 10 bar CO_2 pressure

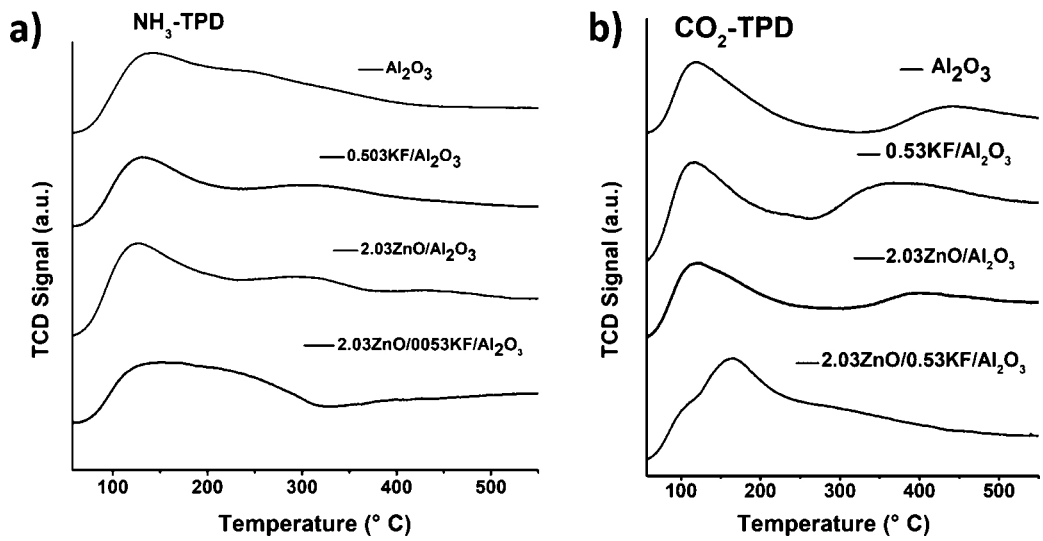

Fig. 6. NH_3- and CO_2-TPD profiles of γ-Al_2O_3, 2.03ZnO/Al_2O_3, 0.53 K F/Al_2O_3 and 2.03ZnO/0.53 K F/Al_2O_3 catalysts.

Table 2
Physicochemical properties and catalyst testing of ZnO/KF/Al_2O_3 catalyst calcined at different temperatures.

Calcination temperature (°C)	Surface area (m^2/g)	Acidity (mmol/g)	Basicity (mmol/g)	Total acid-base sites (mmol/g)	Reaction result			
					Conv. of EDA (%)	Sel. for cyclic urea (%)	Yield of cyclic urea (%)	[a]Yield of major side product (%)
450	137.1	0.26	0.12	0.38	68.6	96.5	66.2	2.0
550	133.4	0.23	0.13	0.36	72.9	98.0	71.4	1.3
650	131.0	0.17	0.14	0.31	65.0	98.6	64.1	0.8
750	126.8	0.14	0.16	0.30	63.2	97.4	61.5	1.4

Reaction condition: 1.2 g of EDA, 10 wt. % of catalyst w.r.t EDA, 10 bar CO_2 pressure, 160 °C, 4 h, 3.2 g of methanol as solvent. [a]methylimidazolidin-2-one.

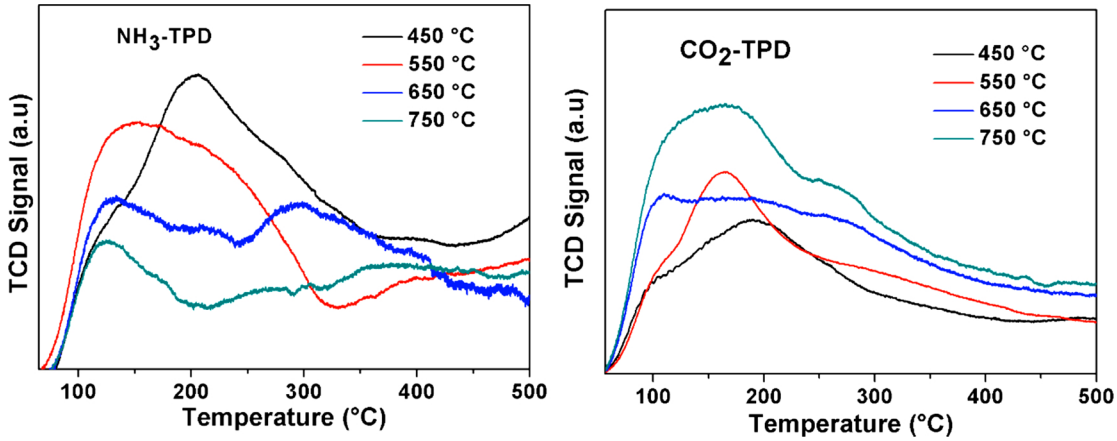

Fig. 7. NH_3 and CO_2-TPD profiles of ZnO/KF/Al_2O_3 catalyst calcined at different temperatures.

(Fig. 14). The increase in reaction time from 2 to 4 h, increased EDA conversion from 23 to 96 % and then there was a slight increase further at longer hours. The selectivity for 2-imidazolidinone was 97 % at 2 h reaction which decreased slightly with an increase in reaction time due to the formation of side product methylimidazolidin-2-one.

3.2.2. *Catalyst leaching and reusability studies*

Recyclability experiments for ZnO/KF/Al_2O_3 catalyst were carried out under 160 °C, 10 bar pressure (CO_2: EDA = 2) and 4 h reaction (Fig. 15a). After fresh catalyst condition, there was a marginal decrease of conversion by 3% which is probably due to the deactivation of those active sites which could not be regenerated with the regeneration procedure. Further, the activity remained almost the same with negligible 0.2–1.5 % variation in the yield compared with 2nd cycle. The leaching test was carried out for ZnO/KF/Al_2O_3 catalyst to understand if any active species are leached out into the reaction medium. It is observed that there is a negligible increase in conversion till 4 h reaction after removing the catalyst from the reaction mixture (Fig. 15b and c). AAS elemental analysis for Zn and K was conducted for the reaction mixture to find if any active species are leached out into the reaction medium. The result showed that both the concentrations of Zn and K were < 1 ppm in the reaction mixture. This confirms the heterogeneity of the catalyst for the reaction of EDA and CO_2.

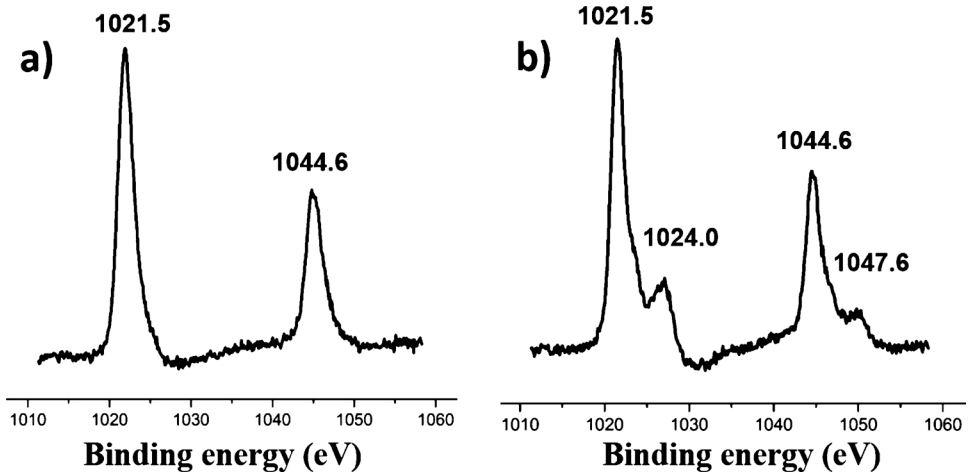

Fig. 8. XPS spectra of Zn 2p a) 2.03ZnO/Al_2O_3 and b) 2.40ZnO/0.49 K F/Al_2O_3 catalyst.

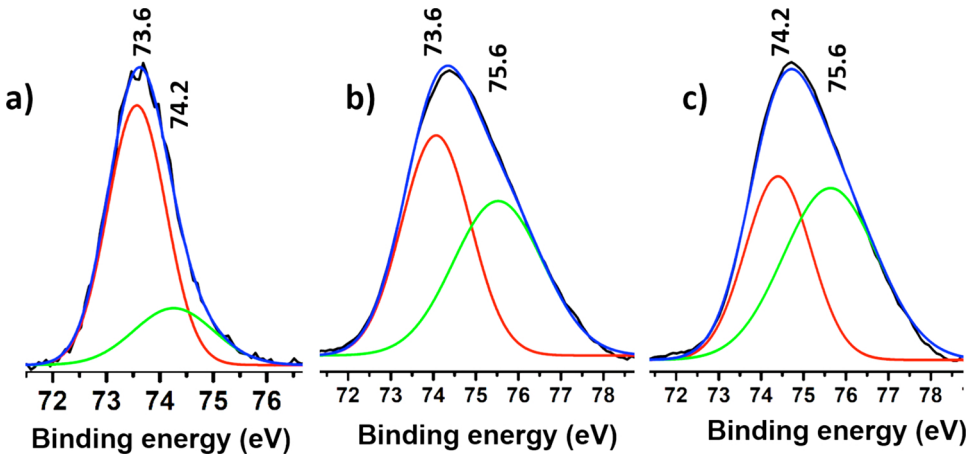

Fig. 9. XPS spectra of Al 2p of a) 2.03ZnO/Al_2O_3 b) 0.53 K F/Al_2O_3, and c) 2.40ZnO/0.49 K F/Al_2O.

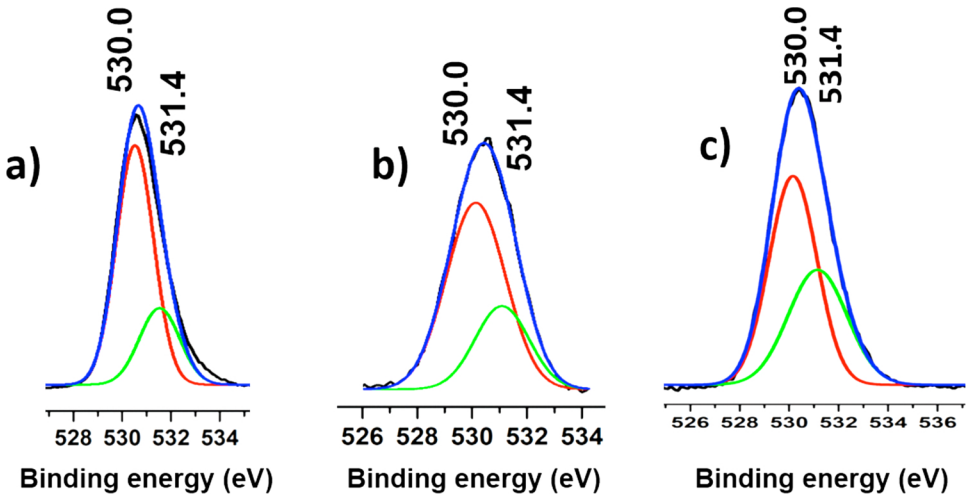

Fig. 10. XPS O 1s spectra of a) 0.53KF/Al_2O_3 b) 2.03ZnO/Al_2O_3 and 3) 2.40ZnO/0.49 K F/Al_2O_3 catalysts.

3.2.3. Solvent effect

The effect of solvent for the synthesis of 2-imidazolidinone was studied under the best reaction condition. Polar protic solvents like alcohols (methanol, ethanol and 1-Propanol) showed better catalytic performance than aprotic polar solvents like DMF, acetonitrile, 1, 2-dichloroethane, and chloroform. However, there was no correlation of dielectric constants of the solvents with catalytic activity as shown in Table 3. Hence, we were prompted to look into other properties of solvents responsible for enhancing the catalytic activity for this reaction. One such property is acceptor and donor numbers which represent acidic and basic properties of the solvent respectively [35–38]. The correlation with this property shows that the solvent with high acceptor number influences the 2-imidazolidinone yield, whereas the solvent with high donor number (DMF) gave least conversion probably due to

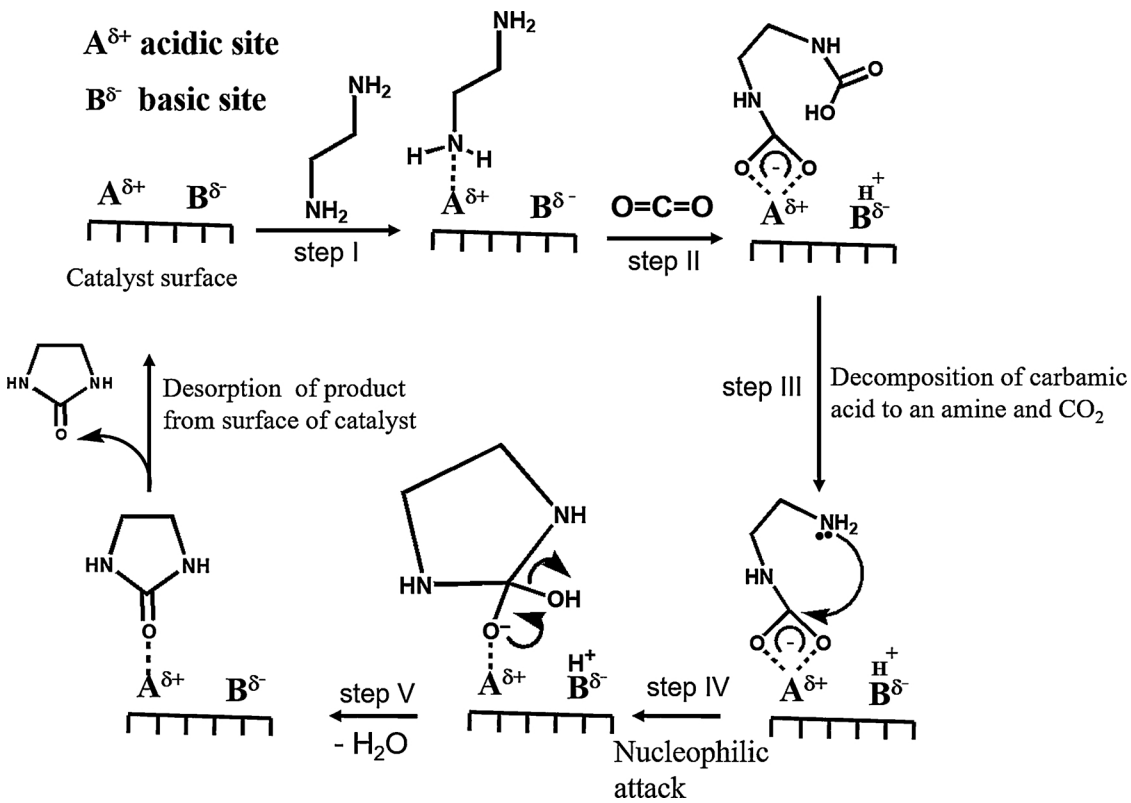

Scheme 1. Plausible mechanism of 2-imidazolidinone from ethylenediamine and CO_2.

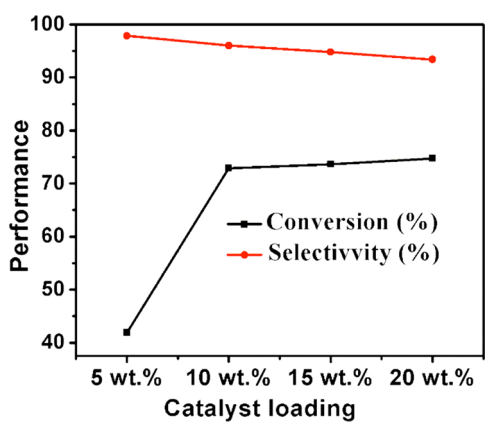

Fig. 11. Effect of catalyst loading, reaction condition: 1.2 g of EDM, 10 bar CO_2 pressure, 160 °C, 4 h, 3.2 g of methanol as solvent, at different wt.% of catalyst w.r.t. EDA.

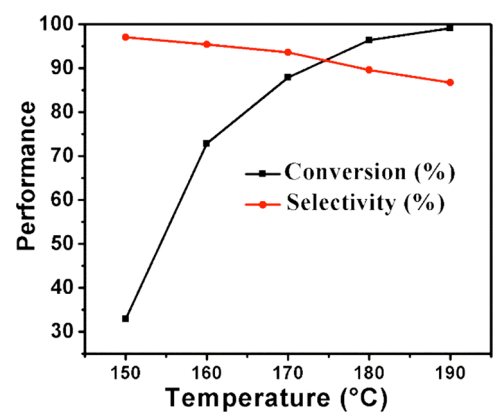

Fig. 12. Effect of temperature, reaction condition: 1.2 g of EDM, 10 wt.% of catalyst w.r.t. EDA, 10 bar CO_2 pressure, 4 h, 3.2 g of methanol as solvent.

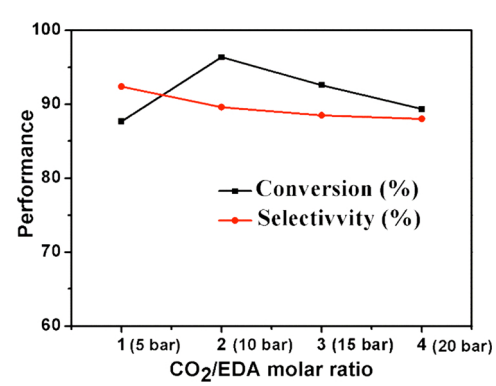

Fig. 13. Effect of pressure, reaction condition: 1.2 g of EDM, 10 wt.% of catalyst w.r.t. EDA, 180 °C, 4 h, 3.2 g of methanol as solvent.

its basic nature which might have blocked the acidic active sites of the catalyst. Each solvent produced different side products due to the side reaction of the solvent itself with either main product or the reactant EDA as mentioned in Table 3. It can be seen that minimum side products were formed with alcohol as a solvent compared to aprotic solvents tested in this study. Among these, methanol, an inexpensive and comparatively less toxic solvent, gave highest 2-imidazolidinone yield (86.3 %).

3.2.4. The reaction of CO_2 with various amines and comparison with CeO_2 catalyst

Different amines were tested by reacting with CO_2 to understand the effectiveness and general applicability of the catalyst. For simplicity, the same reaction condition was used for all the reactions mentioned in Table 4 and the solvent for each reaction was selected as per the

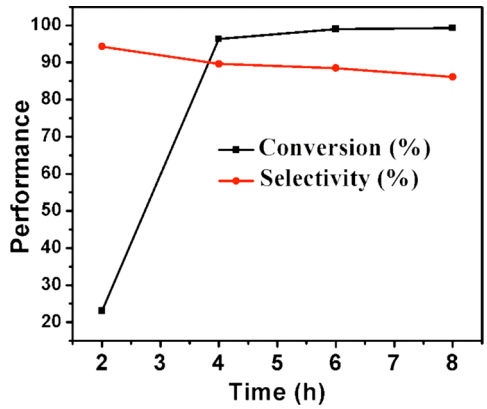

Fig. 14. Effect of time, reaction condition: 1.2 g of EDM, 10 wt. % of catalyst w.r.t. EDA, 180 °C, 10 bar CO_2 pressure, 3.2 g of methanol as solvent.

previous literature [17,18]. The carbonylation of n-butylamine with CO_2 using $ZnO/KF/Al_2O_3$ catalyst resulted in 68.7 % conversion and 93.3 % of selectivity for 1,3-disubstituted urea. The reaction of ethanolamine and CO_2 gave 86.5 % conversion and 93.4 % selectivity for 2-oxazolidinone. On the other hand, diethylamine and aniline gave only trace conversions, which could be because the reactions of CO_2 with these substrates are limited by equilibrium. Earlier report suggests that using a dehydrating agent like 2-cyanopyridine enhanced the catalytic activity for the synthesis of DPU using diethylamine and aniline by driving the reaction forward with the removal of byproduct water [18]. Dehydrating agents have been used previously to enhance the catalytic activity with effective removal of water for equilibrium limited reactions [39–44].

The performance of the catalyst was compared with the best reported catalyst in the literature, CeO_2 for cyclic urea synthesis (Table 4). The catalyst CeO_2 gave 84.5 % of EDA conversion which is 11.8 % lower compared to $ZnO/KF/Al_2O_3$ catalyst, whereas the selectivity for 2-imidazolidinone was 5.8 % higher for CeO_2. The overall activity of $ZnO/KF/Al_2O_3$ is better than CeO_2 under same reaction condition. In previous studies, the CeO_2 catalyst was reported to give 72 % yield for 1,3-dibutyl urea and 97 % yield for 2-oxazolidinone for n-butyl amine and ethanolamine substrates respectively under 50 bar CO_2 pressure, 160 °C and 4 h reaction time [17,18]. For 1,3-diaminopropane, CeO_2 catalyst gave 90 % of yield corresponding to six membered ring urea under 5 bar CO_2 pressure at 160 °C for 24 h [1].

3.2.5. FT-IR adsorption study and plausible mechanism

The FT-IR adsorption study gave some insight on the mechanism on $ZnO/KF/Al_2O_3$ catalyst for the synthesis of 2-imidazolidinone (cyclic urea) from EDA and CO_2 (Fig. 16). For this study, pre-activated 0.53 K F/Al_2O_3, 2.03ZnO/Al_2O_3 and 2.40ZnO/0.49 K F/Al_2O_3 catalysts were adsorbed with EDA and then dried at 160 °C for 30 min to remove physisorbed species before the FT-IR analysis. The 0.53 K F/Al_2O_3 catalyst showed a peak at 1560cm^{-1}, whereas 2.03ZnO/Al_2O_3 and 2.40ZnO/0.49 K F/Al_2O_3 catalysts exhibited at 1572 cm^{-1} corresponding to N−H bending vibration of adsorbed EDA species (Fig. 16. The basic KF/Al_2O_3 contains small number acidic of Al^{3+}, whereas 2.03ZnO/Al_2O_3 possesses predominantly Zn^{2+} acidic centers. The result indicates that EDA could be coordinatively adsorbed on the Al^{3+} acid sites in KF/Al_2O_3, whereas in 2.03ZnO/Al_2O_3 and 2.40ZnO/0.49 K F/Al_2O_3, it could be predominantly adsorbed on Zn^{2+} centers. The introduction of CO_2 onto EDA treated catalysts in the second step (Fig. 16c) shows changes in the FT-IR spectra due to an interaction of CO_2 with EDA. A new band at 1635cm^{-1} [2] was observed in ZnO/Al_2O_3 and $ZnO/KF/Al_2O_3$ catalysts which can be assigned to carbamate adspecies. However, this band is minor in 0.53 K F/Al_2O_3 due to low amount of EDA chemisorbed in the 1st step. The C–H bending vibration of EDA was shifted from 1456 to 1480 cm-1 upon its adsorption on the catalyst which could be because of coordinately bonded amine on the acidic site of the catalyst. Overall, FT-IR reactant adsorption study indicates that Zn^{2+} acid centers could be mainly responsible for the activation of amine for this reaction and also carbamate species could be the possible intermediate from the reaction of CO_2 with chemisorbed EDA on the catalyst.

The plausible reaction mechanism for the synthesis of 2-imidazolidinone from EDA and CO_2 is shown in Scheme 1. From FT-IR studies, EDA predominately adsorbed on Zn^{2+} acid sites. The XPS analysis indicates the presence of higher concentration of $O^{\delta-}$ defect sites formed due to the interaction of ZnO and KF on the Al_2O_3 support. Introduction of CO_2 on the EDA treated catalyst indicated the formation of carbamate species by FTIR study. EDA is known to react with CO_2 even at room temperature to give dicarbamic acid [1]. The basic site on the catalyst abstracts the proton from the carbamic acid group which helps in the formation of carbamate species on the acid site (like Zn^{2+}) as shown in Scheme 1. The free carbamic acid group then decomposes into amine and CO_2 in the third step. In the fourth step, the nucleophilic

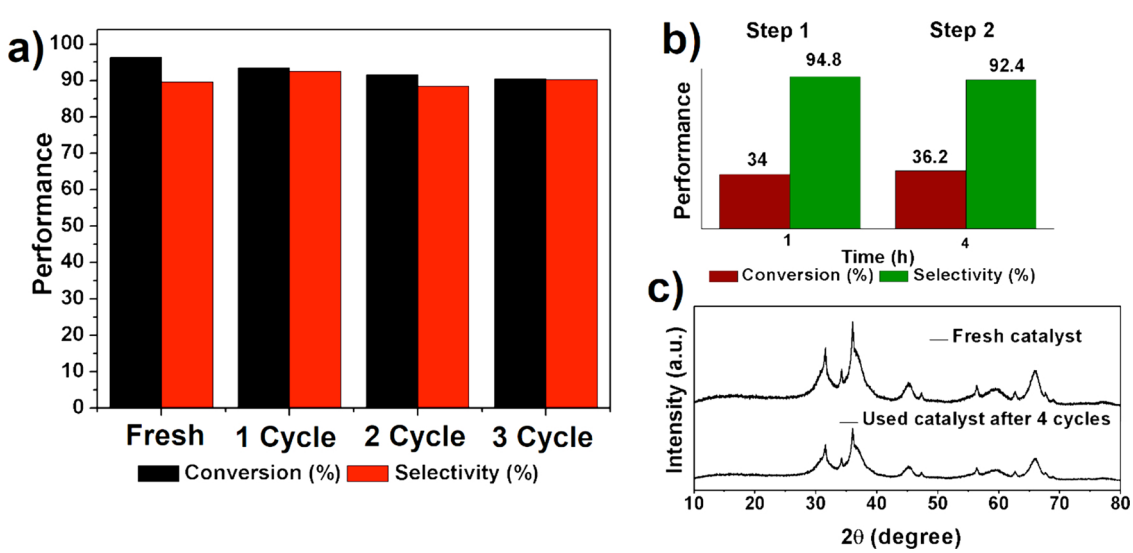

Fig. 15. a) Reusability studies; condition: 180 °C, 1.2 g of EDA, 0.12 g catalyst, 10 bar CO_2, 4 mL of methanol, 4 h; b) Catalyst leaching test: Step 1, 160 °C, 1.2 g of EDA, 0.12 g catalyst, 10 bar CO_2, 4 mL of methanol, 1 h. Step 2: Blank run with the filtrate for 4 h under conditions same as Step 1; c) XRD powder patterns of fresh and used catalyst after 4 cycles.

Table 3
Effect of solvent studies for the synthesis of 2-imidazolidinone from ethylenediamine and CO_2.

SI. No	Solvent	Dielectric constant	Acceptor number (A.N)	Donor number (D.N)	Conv. (%)	cyclic urea selectivity (%)	major Side product selectivity (%)	cyclic urea yield (%)
1	Methanol	32.6	41.3	19.0	96.3	89.6	9.4[a]	86.3
2	Ethanol	22.4	37.1	19.0	93.5	87.7	11.5[b]	82.0
3	1-Propanol	18.0	33.8	21.1	89.3	90.1	8.3[c]	80.5
4	Chloroform	4.8	19.4	3.5	53.5	41.3	16.8[d]	22.1
5	Acetonitrile	36.0	18.9	14.1	95.2	28.4	47.1[e]	27.0
6	1,2-DCE	10.1	16.7	3.2	96.3	29.6	38.4[f]	28.5
7	DMF	36.7	16.0	27.0	20.1	68.6	14.9 [g]	13.8

Reaction condition: 1.2 g of EDA, 10 wt. % of catalyst w.r.t EDA, 10 bar CO_2 pressure, 180 °C, 4 h, 3.2 g of solvent. [a]methylimidazolidin-2-one, [b]ethylimidazolidin-2-one, [c]propylimidazolidin-2-one, [d]unknown, [e]N,N'-diacetylethylenediamine, [f]unknown, [g]1,2-ethylene-bis(formamide).

Table 4
The activity comparison of $ZnO/KF/Al_2O_3$ with CeO_2 catalyst and reaction of various amines with CO_2.

SI. No.	Catalyst	Reactant	Product	Solvent	Conv. (%)	Sel. to product (%)	Activity (mmol/g)
1	CeO_2	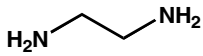	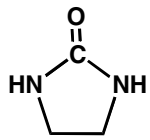	Methanol	84.5	95.4	140.8
2	2.40ZnO /0.49 K F/Al_2O_3	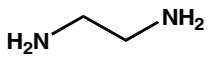	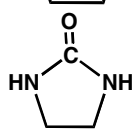	Methanol	96.3	89.6	160.5
3	2.40ZnO /0.49 K F/Al_2O_3	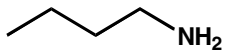	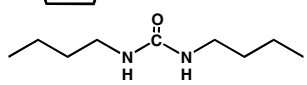	NMP	68.7	94.3	114.5
4	2.40ZnO /0.49 K F/Al_2O_3	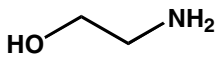	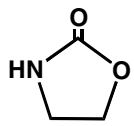	Acetonitrile	86.5	93.4	144.2
5	2.40ZnO /0.49 K F/Al_2O_3	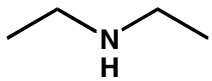	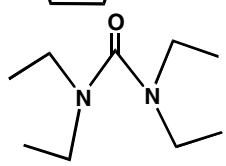	NMP	Trace	Trace	–
6	2.40ZnO /0.49 K F/Al_2O_3	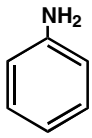	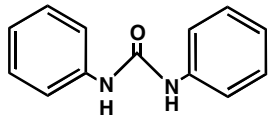	NMP	Trace	Trace	–

Reaction condition: 20 mmol of amine, 10 wt. % of catalyst w.r.t amine, 10 bar CO_2 pressure, 180 °C for 4 h, 3.2 g of solvent. Activity = moles of reactant converted per gram of catalyst.

addition of amine group to the carbonyl carbon of the carbamate group results in 2-imidazolidinone product and the formation of H_2O as a byproduct.

4. Conclusions

In this work, $ZnO/KF/Al_2O_3$ catalyst was prepared by impregnation of ZnO and KF on Al_2O_3 support. The catalytic activity of $ZnO/KF/Al_2O_3$ was higher than that of ZnO/Al_2O_3 and KF/Al_2O_3. Acidic and basic sites in the $ZnO/KF/Al_2O_3$ were tuned by changing the concentration of ZnO and KF on Al_2O_3 support. The catalyst contained rod-like γ-Al_2O_3 and spherical ZnO morphologies with acid-base bifunctional property. Calcination temperature plays an important role in generating active sites and hence influences catalytic activity. Increase in ZnO loading on KF/Al_2O_3 increased both acidity and basicity after an initial decrease in active sites with first loading. Increase in concentration of KF in $ZnO/KF/Al_2O_3$ decreased acidity but increased the basicity which is due to the formation of F^- and OH^- on the Al_2O_3 support. N_2 sorption isotherm confirms that mesoporosity was retained in the $ZnO/KF/Al_2O_3$ catalyst even after the formation of K_3AlF_6 phase on mesoporous Al_2O_3 support. The solvent with high acceptor number influenced the 2-imidazolidinone yield, whereas the solvent with high donor number was found to be unfavorable for the reaction. Optimization of catalyst composition results indicates that acidic and basic sites created by a combination of ZnO and KF on Al_2O_3 are required to get the best catalytic activity in cycloaddition of CO_2 with amines. The catalyst is shown to be stable and reusable by achieving 96.3 % conversion of EDA and 89.6 % selectivity towards the 2-imidazolidinone under optimized reaction conditions. The reaction of various types of amines with CO_2 under identical conditions showed

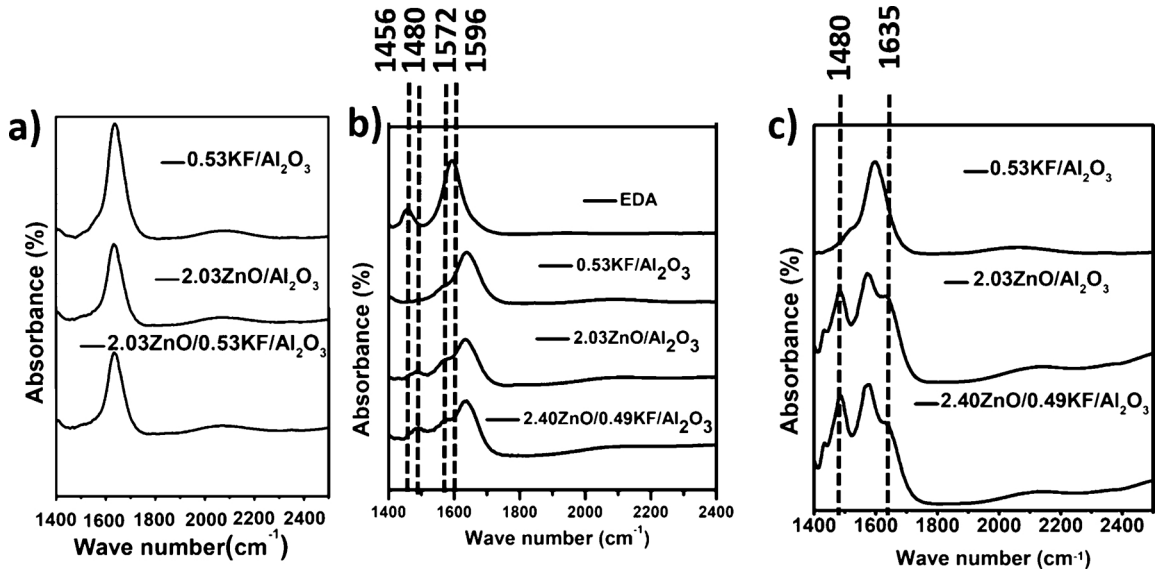

Fig. 16. FT-IR spectra of a) 0.53 K F/Al_2O_3, 2.03ZnO/Al_2O_3 and 2.40ZnO/0.49 K F/Al_2O_3 catalysts before adsorption b) 0.53 K F/Al_2O_3, 2.03ZnO/Al_2O_3 and 2.40ZnO/0.49 K F/Al_2O_3 catalysts after EDA chemisorption c) After CO_2 introduction on EDA chemisorbed catalysts mentioned in b).

that the catalyst works well for diamine, aliphatic amine and amino alcohol, whereas least conversions were obtained for secondary amine and aromatic amine.

Authorship contribution

Conception and design of the study: Ganapati V. Shanbhag acquisition of data: Nagendra Kulal and Crowny John

Analysis and/or interpretation of data: Nagendra Kulal and Ganapati V. Shanbhag

Drafting the manuscript: Nagendra Kulal revising the manuscript critically for important intellectual content: Ganapati V. Shanbhag

Approval of the version of the manuscript to be published (the names of all authors must be listed): Nagendra Kulal, Crowny John and Ganapati V. Shanbhag.

Declaration of Competing Interest

The authors declare that there are no conflicts of interest.

Acknowledgements

GVS thanks Vision Group on Science and Technology, Govt. of Karnataka, India for sponsoring the project under Centre of Excellence in Science Engineering and Medicine (CESEM) Grant (GRD No. 307). The authors acknowledge STIC Cochin University of Science and Technology, Cochin, India for TEM characterization.

Appendix A. Supplementary data

Supplementary material related to this article can be found, in the online version, at doi:https://doi.org/10.1016/j.apcata.2020.117550.

References

[1] M. Tamura, K. Noro, M. Honda, Y. Nakagawa, K. Tomishige, Green Chem. 15 (2013) 1567–1577.
[2] H.F. Wayne, V.G. Theodore, Ethylene urea derivatives, Google Patents, 1945.
[3] D. Frain, F. Kirby, P. McArdle, P. O'Leary, Org. Chem. Int. 2012 (2012).
[4] S.-i. Fujita, H. Kanamaru, H. Senboku, M. Arai, Int. J. Mol. Sci. 7 (2006) 438–450.
[5] K. Kondo, S. Yokoyama, N. Miyoshi, S. Murai, N. Sonoda, Angew. Chem. 18 (1979) 691-691.
[6] W.J. Flosi, D.A. DeGoey, D.J. Grampovnik, H.-j. Chen, L.L. Klein, T. Dekhtyar, S. Masse, K.C. Marsh, H.M. Mo, D. Kempf, Bioorg. Med. Chem. 14 (2006) 6695–6712.
[7] M.-k. Leung, J.-L. Lai, K.-H. Lau, H.-h. Yu, H.-J. Hsiao, J. Org. Chem. 61 (1996) 4175–4179.
[8] R. Nomura, Y. Hasegawa, M. Ishimoto, T. Toyosaki, H. Matsuda, J. Org. Chem. 57 (1992) 7339–7342.
[9] T. Kimura, K. Kamata, N. Mizuno, Angew. Chem. 51 (2012) 6700–6703.
[10] B.M. Bhanage, S.-i. Fujita, Y. Ikushima, M. Arai, Green Chem. 5 (2003) 340–342.
[11] C. Wu, H. Cheng, R. Liu, Q. Wang, Y. Hao, Y. Yu, F. Zhao, Green Chem. 12 (2010) 1811–1816.
[12] D.-L. Kong, L.-N. He, J.-Q. Wang, Synlett 2010 (2010) 1276–1280.
[13] A. Primo, E. Aguado, H. Garcia, ChemCatChem 5 (2013) 1020–1023.
[14] K. Tomishige, M. Tamura, Y. Nakagawa, Chem. Rec. (2018).
[15] M. Tamura, M. Honda, Y. Nakagawa, K. Tomishige, J. Chem. Technol. 89 (2014) 19–33.
[16] M. Honda, S. Sonehara, H. Yasuda, Y. Nakagawa, K. Tomishige, Green Chem. 13 (2011) 3406–3413.
[17] M. Tamura, M. Honda, K. Noro, Y. Nakagawa, K. Tomishige, J. Catal. 305 (2013) 191–203.
[18] M. Tamura, K. Ito, Y. Nakagawa, K. Tomishige, J. Catal. 343 (2016) 75–85.
[19] M. Tamura, A. Miura, M. Honda, Y. Gu, Y. Nakagawa, K. Tomishige, ChemCatChem 10 (2018) 4821–4825.
[20] K.A. Alferov, Z. Fu, S. Ye, D. Han, S. Wang, M. Xiao, Y. Meng, ACS Sustain. Chem. Eng. 7 (2019) 10708–10715.
[21] C. Xu, J. Sun, B. Zhao, Q. Liu, Appl. Catal. B 99 (2010) 111–117.
[22] L.M. Weinstock, J.M. Stevenson, S.A. Tomellin, S.-H. Pan, T. Utne, R.B. Jobson, D.F. Reinhold, Tetrahedron Lett. 27 (1986) 3845–3848.
[23] X. Bo, X. Guomin, C. Lingfeng, W. Ruiping, G. Lijing, Energy Fuels 21 (2007) 3109–3112.
[24] Y. Tang, H. Ren, F. Chang, X. Gu, J. Zhang, RSC Adv. 7 (2017) 5694–5700.
[25] T. Ando, J.H. Clark, D.G. Cork, T. Hanafusa, J. Ichihara, T. Kimura, Tetrahedron Lett. 28 (1987) 1421–1424.
[26] L. Samain, A. Jaworski, M. Edén, D.M. Ladd, D.-K. Seo, F.J. Garcia-Garcia, U. Häussermann, J. Solid State Chem. 217 (2014) 1–8.
[27] K. Tanabe, K. Shimazu, H. Hattori, K. Shimazu, J. Catal. 57 (1979) 35–40.
[28] N. Mintcheva, A. Aljulaih, W. Wunderlich, S. Kulinich, S. Iwamori, Materials 11 (2018) 1127.
[29] D. Zhang, Q. Guo, Y. Ren, C. Wang, Q. Shi, Q. Wang, X. Xiao, W. Wang, Q. Fan, J. Solgel Sci. Technol. 85 (2018) 121–131.
[30] X. Duan, D. Yuan, F. Yu, Inorg. Chem. 50 (2011) 5460–5467.
[31] G. Mattogno, G. Righini, G. Montesperelli, E. Traversa, Appl. Surf. Sci. 70 (1993) 363–366.
[32] G. McGuire, G.K. Schweitzer, T.A. Carlson, Inorg. Chem. 12 (1973) 2450–2453.
[33] J.-C. Dupin, D. Gonbeau, P. Vinatier, A. Levasseur, Phys. Chem. Chem. Phys. 2 (2000) 1319–1324.
[34] R. Andreeva, E. Stoyanova, A. Tsanev, D. Stoychev, Chem. Commun. 48 (2016) 96–102.
[35] I. Persson, Pure Appl. Chem. 58 (1986) 1153–1161.
[36] V.S. Marakatti, G.V. Shanbhag, A. Halgeri, Appl. Catal. A Gen. 451 (2013) 71–78.
[37] M.A. Fard, G. Rounaghi, M. Chamsaz, K. Taheri, J. Inclusion Phenomena Macrocyclic Chem. 64 (2009) 49–56.
[38] J.A. Caram, M. Banera, J.M. Suárez, M.V. Mirifico, Electrochim. Acta 249 (2017) 431–445.
[39] M. Honda, S. Kuno, N. Begum, K.-i. Fujimoto, K. Suzuki, Y. Nakagawa,

K. Tomishige, Appl. Catal. A Gen. 384 (2010) 165–170.
[40] M. Honda, M. Tamura, Y. Nakagawa, S. Sonehara, K. Suzuki, Ki. Fujimoto, K. Tomishige, ChemSusChem 6 (2013) 1341–1344.
[41] M. Honda, A. Suzuki, B. Noorjahan, K.-i. Fujimoto, K. Suzuki, K. Tomishige, Chem. Commun. (2009) 4596–4598.
[42] M. Honda, M. Tamura, Y. Nakagawa, K. Nakao, K. Suzuki, K. Tomishige, J. Catal. 318 (2014) 95–107.
[43] M. Honda, S. Kuno, S. Sonehara, Ki. Fujimoto, K. Suzuki, Y. Nakagawa, K. Tomishige, ChemCatChem 3 (2011) 365–370.
[44] Y. Gu, A. Miura, M. Tamura, Y. Nakagawa, K. Tomishige, ACS Sustain. Chem. Eng. 7 (2019) 16795–16802.